

See discussions, stats, and author profiles for this publication at: <https://www.researchgate.net/publication/7865949>

Lateral Nanopatterns in Thin Diblock Copolymer Films Induced by Selective Solvents

ARTICLE *in* LANGMUIR · MAY 2004

Impact Factor: 4.46 · DOI: 10.1021/la0360815 · Source: PubMed

CITATIONS

45

READS

22

4 AUTHORS, INCLUDING:



Zhijun Hu

Soochow University (PRC)

61 PUBLICATIONS 1,210 CITATIONS

SEE PROFILE

Notes

Lateral Nanopatterns in Thin Diblock Copolymer Films Induced by Selective Solvents

Yongzhong Chen, Haiying Huang, Zhijun Hu, and
Tianbai He*

State Key Laboratory of Polymer Physics and Chemistry,
Changchun Institute of Applied Chemistry,
Chinese Academy of Sciences,
Changchun, 130022, People's Republic of China

Received November 5, 2003.
In Final Form: February 19, 2004

Introduction

Block copolymers have long been studied for their theories and applications especially in nanotechnology.^{1–5} They have periodic structures with 10–100 nm long microphase separated domains which can be controlled by the molecular weight and composition of the block copolymer. Regulating these two parameters, one can prepare thin films with different morphologies over large areas. The patterns formed by the diblock copolymers could be used as templates for structures on the scale of tens to hundreds of nanometers. For the exploitation of block copolymer thin films especially in nanotechnology, the nanopatterns of films with perfectly ordered domains over large areas are prerequisite; therefore, many efforts are focused on controlling the orientation and perfection of ordering of the domains in thin films.⁶

Interfacial energies^{7–11} and commensurability^{12,13} determine the behavior of block copolymer thin films. Thus, changing interfacial energies is a general approach for preparing block copolymer films with perfect ordered domains. For instance, Russell and co-workers used random copolymer brushes to tune the interactions of

symmetric and asymmetric polystyrene-*b*-poly(methyl methacrylate) (PS-*b*-PMMA) copolymers with their boundaries to achieve perpendicular orientation of domains in thin block copolymer films,^{5,14} and this way is usually combined with electric fields.^{14d} Electric fields were used to overcome interfacial interactions to orient nanoscopic domains within diblock copolymer films.¹⁵ Rockford et al. and Yang et al. employed chemically heterogeneous substrates to control nanoscale surface interactions and subsequent macromolecular ordering.^{6,16} Segalman et al. demonstrated graphoepitaxy to produce thin film arrays of spherical block copolymer with good long-range order.¹⁷ Fasolka et al. reported the use of the dependence of morphologies on the film thickness together with corrugated substrates by which the lateral nanometer scale patterning of diblock copolymer films was gained.¹⁸ Spatz et al. demonstrated the formation of surface-induced nanopattern in ultrathin polystyrene-*b*-poly(2-vinylpyridine) (PS-*b*-P2VP) films caused by strong adsorption of one of the two blocks forming a quasi-two-dimensional coil while the other block dewets this adsorption layer.^{19,20}

All the above routes obtaining laterally ordered microdomain structures in thin polymer films need thermal treatment. Recently, other nonequilibrium ways have been noted. The adsorption of diblock copolymers from a selective solvent onto a flat solid substrate results in the formation of laterally ordered microdomains.^{21–24} Apart from these, the solvent-influenced ordering has been used

* To whom correspondence should be addressed. E-mail: tbhe@ciac.jl.cn.

(1) Hamley, I. W. *The Physics of Block Copolymers*; Oxford University Press: Oxford, 1998.

(2) Bates, F. S.; Fredrickson, G. H. *Annu. Rev. Phys. Chem.* **1990**, *41*, 525.

(3) Park, M.; Harrison, C.; Chaikin, P. M.; Register, R. A.; Adamson, D. H. *Science* **1997**, *276*, 1401.

(4) Thurn-Albrecht, T.; Schotter, J.; Kastle, G. A.; Emley, N.; Shibauchi, T.; Krusin-Elbaum, L.; Guarini, K.; Black, C. T.; Tuominen, M. T.; Russell, T. P. *Science* **2000**, *290*, 2126.

(5) Jeong, U.; Kim, H.; Rodriguez, R. L.; Tsai, I. Y.; Stafford, C. M.; Kim, J. K.; Hawker, C. J.; Russell, T. P. *Adv. Mater.* **2002**, *14*, 274.

(6) (a) Yang, X. M.; Peters, R. D.; Nealey, P. F.; Solak, H. H.; Cerrina, F. *Macromolecules* **2000**, *33*, 9575. (b) Kim, S. O.; Solak, H. H.; Stoykovich, M. P.; Ferrier, N. J.; de Pablo, J. J.; Nealey, P. F. *Nature* **2003**, *424*, 411.

(7) Huang, E.; Mansky, P.; Russell, T. P.; Harrison, C.; Chaikin, P. M.; Register, R. A.; Hawker, C. J.; Mays, J. *Macromolecules* **2000**, *33*, 80.

(8) Hasegawa, H.; Hashimoto, T. *Macromolecules* **1985**, *18*, 589.

(9) Fredrickson, G. H. *Macromolecules* **1987**, *20*, 2535.

(10) Hanke, C.; Thomas, E. L.; Fetters, L. J. *J. Mater. Sci.* **1988**, *23*, 1685.

(11) Anastasiadis, S. H.; Russell, T. P.; Satija, S. K.; Majkrzak, C. F. *J. Chem. Phys.* **1990**, *92*, 5677.

(12) Coulon, G.; Deline, V. R.; Russell, T. P.; Green, P. F. *Macromolecules* **1989**, *22*, 2581.

(13) Anastasiadis, S. H.; Russell, T. P.; Satija, S. K.; Majkrzak, C. F. *Phys. Rev. Lett.* **1989**, *62*, 1852.

(14) (a) Mansky, P.; Liu, Y.; Huang, E.; Russell, T. P.; Hawker, C. *Science* **1997**, *275*, 1458. (b) Mansky, P.; Russell, T. P.; Hawker, C. J.; Pitsikalis, M.; Mays, J. *Macromolecules* **1997**, *30*, 6810. (c) Huang, E.; Russell, T. P.; Harrison, C.; Chaikin, P. M.; Register, R. A.; Hawker, C. J. *Macromolecules* **1998**, *31*, 7641. (d) Thurn-Albrecht, T.; Steiner, R.; DeRouchey, T.; Stafford, C. M.; Huang, E.; Bal, M.; Tuominen, M.; Hawker, C. J.; Russell, T. P. *Adv. Mater.* **2000**, *12*, 757.

(15) (a) Morkved, T. L.; Lu, M.; Urbas, A. M.; Enrichs, E. E.; Jaeger, H. M.; Mansky, P.; Russell, T. P. *Science* **1996**, *273*, 931. (b) Mansky, P.; DeRouchey, J.; Russell, T. P.; Mays, J.; Pitsikalis, M.; Morkved, T.; Jaeger, H. *Macromolecules* **1998**, *31*, 4399. (c) Thurn-Albrecht, T.; DeRouchey, T.; Russell, T. P.; Jaeger, H. M. *Macromolecules* **2000**, *33*, 3250.

(16) Rockford, L.; Liu, Y.; Mansky, P.; Russell, T. P.; Yoon, M.; Mochrie, S. G. *J. Phys. Rev. Lett.* **1999**, *82*, 2602.

(17) Segalman, R. A.; Yokoyama, H.; Kramer, E. J. *Adv. Mater.* **2001**, *13*, 1152.

(18) Fasolka, M. J.; Harris, D. J.; Mayes, A. M.; Yoon, M.; Mochrie, S. G. *J. Phys. Rev. Lett.* **1997**, *79*, 3018.

(19) (a) Spatz, J. P.; Sheiko, S.; Möller, M. *Adv. Mater.* **1996**, *8*, 513. (b) Spatz, J. P.; Sheiko, S.; Möller, M.; Noeske, M.; Behm, R. J.; Pietralla, M. *Macromolecules* **1997**, *30*, 3874. (c) Spatz, J. P.; Eibeck, P.; Möller, M.; Herzog, T.; Ziemann, P. *Adv. Mater.* **1998**, *10*, 849. (d) Spatz, J. P.; Eibeck, P.; Mössmer, S.; Möller, M.; Kramarenko, E. Y.; Khalatur, P. G.; Potemkin, I. I.; Khokhlov, A. R.; Winkler, R. G.; Reineker, P. *Macromolecules* **2000**, *33*, 150.

(20) (a) Kramarenko, E. Y.; Potemkin, I. I.; Khokhlov, A. R.; Winkler, R. G.; Reineker, P. *Macromolecules* **1999**, *32*, 3495. (b) Potemkin, I. I.; Kramarenko, E. Y.; Khokhlov, A. R.; Winkler, R. G.; Reineker, P.; Eibeck, P.; Spatz, J. P.; Möller, M. *Langmuir* **1999**, *15*, 7290.

(21) (a) Spatz, J. P.; Roescher, A.; Sheiko, S.; Krausch, G.; Möller, M. *Adv. Mater.* **1995**, *7*, 731. (b) Spatz, J. P.; Sheiko, S.; Möller, M. *Macromolecules* **1996**, *29*, 3220. (c) Spatz, J. P.; Roescher, A.; Möller, M. *Adv. Mater.* **1996**, *8*, 337. (d) Spatz, J. P.; Herzog, T.; Mössmer, S.; Ziemann, P.; Möller, M. *Adv. Mater.* **1999**, *11*, 149.

(22) (a) Meiners, J. C.; Ritzi, A.; Rafailovich, M. H.; Sokolov, J.; Mlynek, J.; Krausch, G. *Appl. Phys. A* **1995**, *61*, 519. (b) Meiners, J. C.; Elbs, H.; Ritzi, A.; Mlynek, J.; Krausch, G. *J. Appl. Phys.* **1996**, *80*, 2224. (c) Meiners, J. C.; Ritzi, A.; Mlynek, J.; Elbs, M.; Krausch, G. *Macromolecules* **1997**, *30*, 4945.

to produce a long range ordered film without any thermal treatment.^{25–29} By regulating the solvent evaporation rate, the ordering of thin block copolymer films can be obtained, and usually a neutral solvent is used.³⁰ An advantage of this method is avoiding sample thermodegradation. However, genuinely neutral solvents are rarely found and the solvent selectivity is ubiquitous. We conjecture that if a selective solvent is used in solvent annealing, a quasi-micellar microdomain phase should be formed. In our present work, we have explored structures of thin symmetric and asymmetric PS-*b*-PMMA films in saturated selective solvent vapor. Acetone was selected as a selective solvent for PMMA. It is certain that the structures induced by selective solvents are far from the equilibrium situation, but at room temperature the thin films are stable because the glass transition temperature (T_g) of both PS and PMMA are $\sim 100^\circ\text{C}$. This long-term stability of ordered structures is significant for their applications in nanolithography.²⁶

Experimental Section

Symmetric and asymmetric polystyrene-*b*-poly(methyl methacrylate) (PS-*b*-PMMA) diblock copolymers with (1) SMMA1 ($M_n = 201.5$ kg/mol, $N_{PS} = 899$, $N_{PMMA} = 1080$, polydispersity = 1.19) and (2) SMMA2 ($M_n = 176.7$ kg/mol, $N_{PS} = 1257$, $N_{PMMA} = 460$, polydispersity = 1.10) were purchased from Polymer Source Inc. and used as received.

In the experiment, the diblock copolymers were dissolved in toluene, forming 5 mg/mL solutions of the block copolymers in toluene. Thin PS-*b*-PMMA films were prepared on carbon-coated mica, freshly cleaved mica, and polished silicon substrates spun cast at 3000 rpm from their solutions for 40 s. After drying, the films were immediately put in an airtight glass vessel with 31 cm³ volume with 50 μL of the reservoir acetone at the initiation of the solvent-annealing process. The total pressure was 1.27 atm, and the temperature of the acetone vapor was kept at $\sim 23^\circ\text{C}$. After being exposed for different times to an acetone vapor, the samples were removed from the vessel quickly and dried in air at room temperature ($\sim 23^\circ\text{C}$).

The samples were investigated by means of atomic force microscopy (AFM) using a Nanoscope IIIa (Digital Instruments Inc., Santa Barbara, CA) working in the tapping mode at ambient conditions. Transmission electron microscopy (TEM) was conducted in a JEOL 2010 TEM with an accelerating voltage of 200 kV in the bright-field mode. Because TEM serves to confirm the identity of individual components (i.e., PS or PMMA) in the TM-AFM images, only a subset of samples was studied. Specimens were exposed to RuO₄ vapor for 2 h, which selectively stains the PS block and provides contrast in electron density. The process in which the specimens were transferred to TEM grids might cause a change of the morphologies, but it has little effect on the confirmation of the identity of PS and PMMA domains. After RuO₄ staining, dark regions of the bright-field TEM images are identifiable with the PS domains whereas the bright regions are PMMA. For mica, silicon, and carbon, the results are similar, so we mainly give results on carbon.

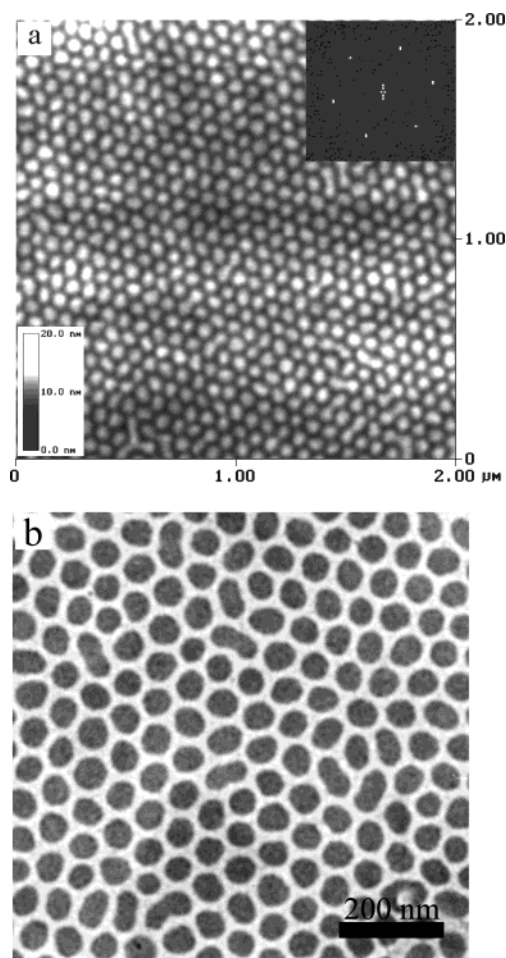


Figure 1. AFM height image (a) and TEM micrograph (b) of thin films of SMMA1 spin-coated from 5 mg/mL toluene solution onto carbon annealed by acetone vapor for 6.5 h. The inset of (a) shows the corresponding fast Fourier transformation (FFT) and height scale.

Results and Discussion

The miscibility between a polymer and a solvent is governed by the polymer–solvent interaction parameter χ_{PS} . Because acetone is a polar solvent, in calculating Flory's interaction parameters, one may consider that the solubility parameter for the polymer or solvent can be separated into two components, a polar solubility parameter and a dispersion solubility parameter. Thus, the expression $\chi_{PS} = V_s[(\delta_{dS} - \delta_{dP})^2 + (\delta_{pS} - \delta_{pP})^2]/RT$ has been used in calculating Flory's interaction parameters,³¹ where V_s is the molar volume of the solvent, R is the gas constant, δ_d is the dispersion solubility parameter, and δ_p is the polar solubility parameter (S = solvent and P = polymer). According to the literature,³² δ_d 's for PS, PMMA, and acetone are respectively 17.6, 18.8, and 15.5 MPa^{1/2}, V_s for acetone is 73.3 cm³, and δ_p 's for PS, PMMA, and acetone are 6.1, 10.2 and 10.4 MPa^{1/2}, respectively. One may then find that, at 300 K (23 $^\circ\text{C}$), χ_{PS} values for PS and PMMA in acetone are 0.624 and 0.321. Furthermore, using the Flory–Huggins criterion for complete solvent–polymer miscibility, i.e., $\chi_{PS} < 0.5$, acetone should be a nonsolvent for PS and a good solvent for PMMA. Thus, acetone is a selective solvent for the PS-*b*-PMMA diblock copolymer.

(31) Chen, S.-A. *J. Appl. Polym. Sci.* **1971**, *15*, 1247.

(32) Van Krevelen, D. W. *Properties of Polymers*; Elsevier Scientific Publishing Company: Amsterdam, Oxford, New York, 1976.

(23) Li, Z.; Zhao, W.; Rafailovich, M. H.; Sokolov, J.; Khougaz, K.; Lennox, B.; Eisenberg, A.; Krausch, G. *J. Am. Chem. Soc.* **1996**, *118*, 10892.

(24) Sohn, B.-H.; Yoo, S.-I.; Seo, B.-W.; Yun, S.-H.; Park, S.-M. *J. Am. Chem. Soc.* **2001**, *123*, 12734.

(25) Fukunage, K.; Elbs, H.; Magerle, R.; Krausch, G. *Macromolecules* **2000**, *33*, 947.

(26) Niu, S.; Saraf, R. F. *Macromolecules* **2003**, *36*, 2428.

(27) Kim, G.; Libera, M. *Macromolecules* **1998**, *31*, 2569.

(28) Knoll, A.; Horvat, A.; Lyakhova, K. S.; Krausch, G.; Sevink, G. J. A.; Zvelindovsky, A. V.; Magerle, R. *Phys. Rev. Lett.* **2002**, *89*, 035501.

(29) Elbs, H.; Drummer, C.; Abetz, V.; Krausch, G. *Macromolecules* **2002**, *35*, 5570.

(30) (a) Zhang, Q.; Tsui, O. K. C.; Du, B.; Zhang, F.; Tang, T.; He, T. *Macromolecules* **2000**, *33*, 9561. (b) Huang, H.; Zhang, F.; Hu, Z.; Du, B.; He, T.; Lee, F. K.; Wang, Y.; Tsui, O. K. C. *Macromolecules* **2003**, *36*, 4084.

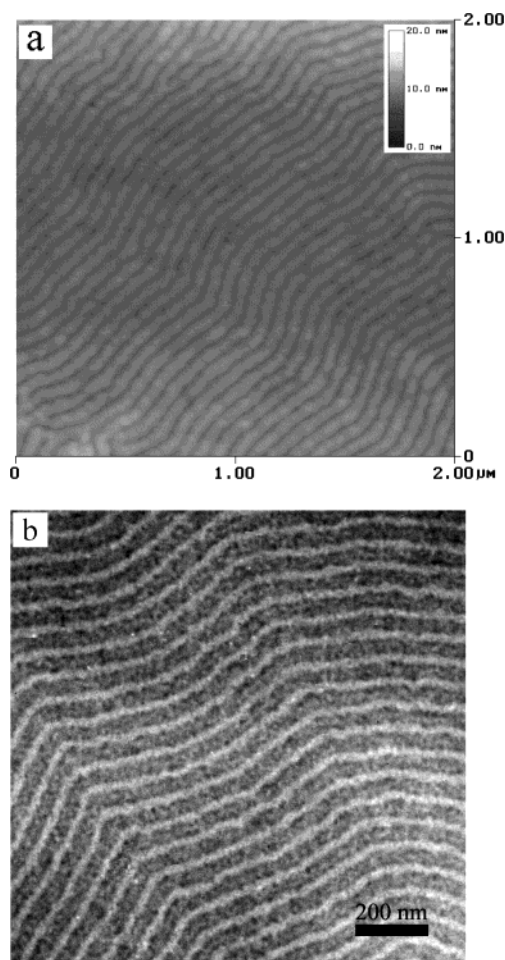


Figure 2. Images of thin film of SMMA1 spin-coated from 5 mg/mL toluene solution onto carbon after annealing in acetone vapor for 12 h: (a) AFM height image; (b) TEM micrograph. The height scale is shown in the inset of (a).

Figures 1 and 2 give AFM images of thin SMMA1 film spun cast from 5 mg/mL toluene solution onto a carbon substrate treated with acetone for different times. When SMMA1 thin films were annealed for 6.5 h, highly ordered hexagonal close packing spherical domains were formed, as depicted in Figure 1. The spacing of the adjacent PS domains is ~ 79.5 nm. In the state of spherical microdomains, the structure is of a core of the insoluble block PS surrounded by a highly stretched corona of the soluble block PMMA, with ~ 2.4 nm average protrusion height. After treating for 12 h in acetone vapor, striped structures were formed, as shown by Figure 2. This structure of striped domains is like that of perpendicular lamellar microdomains of symmetric diblock thin films annealed on a neutral substrate.^{14c} Moreover, for the symmetric PS-*b*-PMMA SMMA1 sample, we found that the lateral period of stripes (~ 67 nm determined by AFM) is nearly identical to the lamellar period of bulk sample L_0 (~ 66 nm calculated from the empirical relation¹¹). The protrusive striped domains are PS phase revealed by AFM and TEM images in Figure 2. The lateral structure may consist of PS cylinders in PMMA matrix or the alternatively perpendicular arrays of PS and PMMA domains absorbed on the underlayer brush.^{22c}

For asymmetric diblock copolymer SMMA2 thin films spin-coated from toluene solutions onto a carbon substrate, when annealed in acetone vapor for 6.5 h, similar quasi-hexagonal close packing domains were also formed, which is clearly shown by the AFM image in Figure 3. The inset

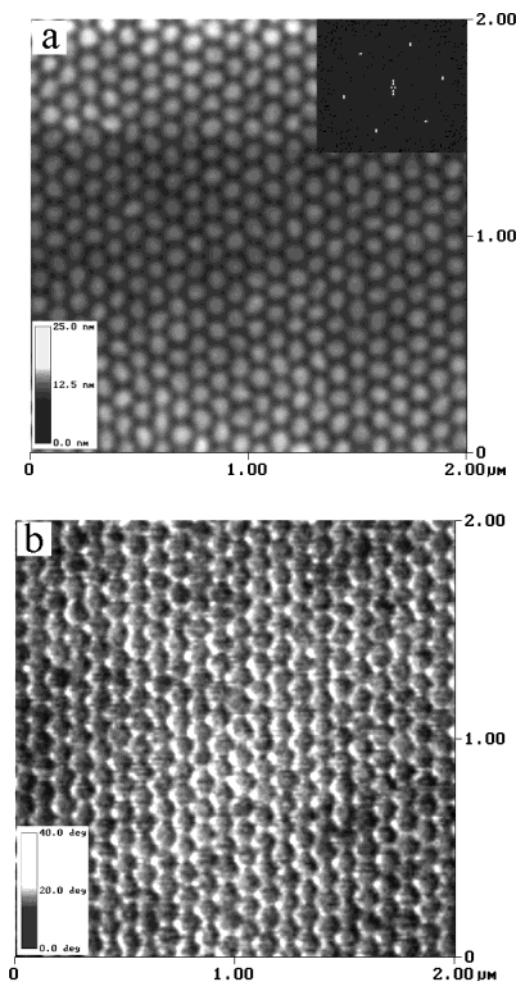


Figure 3. AFM images of thin film of SMMA2 spin-coated from 5 mg/mL toluene solution onto carbon after annealing in acetone vapor at room temperature for 6.5 h: (a) height image; (b) phase image. The FFT, height scale, and phase scale are shown in the inset.

of Figure 3a shows the Fourier transformation (FT) of the image in the main panel of the same figure. The average spacing between every two protrusions in Figure 3 is ~ 105 nm. In the AFM phase image in Figure 3b, the darker areas correspond to the PS domains and the brighter correspond to the PMMA matrix.⁵ Combined with Figure 3b, it is determined that the protrusive domains in the height image in Figure 3a are PS. In comparison with the symmetric diblock copolymer SMMA1, striped structures can also be gained after the asymmetric diblock copolymer SMMA2 thin film annealing in acetone vapor for 24 h, as shown by Figure 4. Similarly, in the AFM phase in Figure 4b, the darker areas represent the PS domains. The lateral spacing is ~ 95 nm, which is larger than that of the bulk period L_0 . However, this distinction between symmetric and asymmetric diblock copolymers has not been well understood.

In the process of the transition from spheres to stripes, there is little or no mass transport of block copolymers. What is changed is only the connectivity with adjacent domains, and the transition process is defined as mordenitic-type phase transitions.³³ It makes long-range order possible by external fields. For obtaining striped domains, the distance between adjacent micelles should be small enough, which affords more probability of coalescence of

(33) Breulmann, M.; Förster, S.; Antonietti, M. *Macromol. Chem. Phys.* **2000**, *201*, 204.

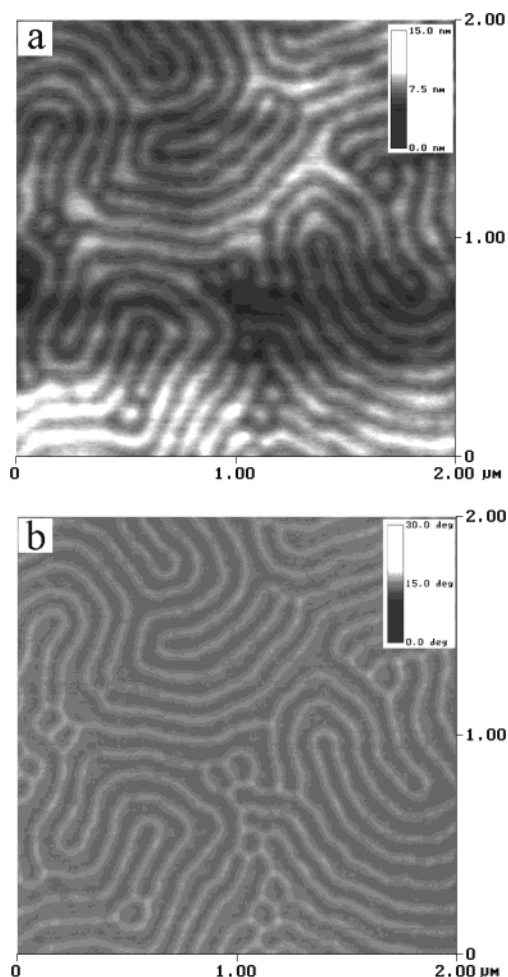


Figure 4. AFM images of thin film of SMMA2 spin-coated from 5 mg/mL toluene solution onto carbon annealed by acetone vapor at room temperature for 24 h: (a) height image; (b) phase image. The height and phase scales are shown in the inset.

spherical domains. Without modifying the structure of block copolymers,³³ or changing polymer concentration,²³ but only changing annealing time, we observed a similar transition from “circular-to-ribbon” shapes as shown in Figures 2 and 4. This may offer a means of achieving different nanostructures of block copolymer thin films. This transition may also take place at elevated temperature,^{22a} but it is not involved in this paper. One of the reasons that cause the change from the sphere to the striped patterns could be the following: For 6.5 h, the

degree of the absorption of acetone is different between PS and PMMA due to the preferentiality of PMMA, but after 12 h, the degree of the absorption reaches the same level in PS and in PMMA. Therefore, the film shows the same pattern as their bulks.

Another question is that of how the order of thin films could be formed. When PS-*b*-PMMA thin films were spin-coated from solutions, the thin films were disordered. From the disordered state to the ordered one, an entropy penalty is obvious. How could this process occur? When the thin films were exposed to the acetone vapor, the aggregates of the insoluble block (PS) were formed, but in the existence of solvent, the free volume of the soluble block (PMMA) increased much. The penalty in entropy by the ordering process is overcompensated by the gain of free volume of the soluble block. As the solvent is extracted, because of the high viscosity of polymer, the morphologies can be frozen, so the nanopatterns are in fact a kind of frozen-in structure. However, because of the high T_g of both blocks, the ordered structure can remain for a long time at room temperature.

Conclusions

We have developed a highly reproducible and simple means of obtaining nanopatterns in PS-*b*-PMMA diblock copolymer thin films. This method needs a selective solvent for one block, and does not need thermal annealing. In our work, we mainly select acetone as the preferential solvent of the PMMA block in PS-*b*-PMMA. When the PS-*b*-PMMA thin films are annealed by acetone, the highly lateral ordered nanopatterns can be formed with different morphologies from spherical domains to striped ones. The characteristic spacing of striped surface patterns gained from symmetric diblock copolymers is similar to the bulk period L_0 . After solvent extraction, the formed structures are frozen. Both components PS and PMMA are vitrified and stiff at room temperature; therefore, the surface pattern can be stable under ambient conditions. Thus, the stable ordered structures are useful for nanolithographic techniques of fabricating nanostructures on solid substrates. Usually, gaining a lateral surface pattern needs strict commensurability, but the method in this study has overcome this constraint to a certain extent. Another trait is that the ordering is induced on chemically homogeneous substrates over large areas.

Acknowledgment. This work was supported by the National Science Foundation of China.

LA0360815